# Myosin VI and vinculin cooperate during the morphogenesis of cadherin cell–cell contacts in mammalian epithelial cells

Madhavi P. Maddugoda, Matthew S. Crampton, Annette M. Shewan, and Alpha S. Yap

Division of Molecular Cell Biology, Institute for Molecular Bioscience, The University of Queensland, St. Lucia, Brisbane, Queensland 4072, Australia

Cooperation between cadherins and the actin cytoskeleton controls many aspects of epithelial biogenesis. We report here that myosin VI critically regulates the morphogenesis of epithelial cell–cell contacts. As epithelial monolayers mature in culture, discontinuous cell–cell contacts are initially replaced by continuous (cohesive) contacts. Myosin VI is recruited to cell contacts as they become linear and cohesive, where it forms a biochemical complex with epithelial cadherin (E-cadherin). Myosin VI is necessary for strong cadherin adhesion, for cells to form cohesive linear contacts, and for the integrity of the apical junctional complex. We find that vinculin mediates this effect of myosin VI. Myosin VI is necessary for vinculin and E-cadherin to interact. A combination of gain and loss of function approaches identifies vinculin as a downstream effector of myosin VI that is necessary for the integrity of intercellular contacts. We propose that myosin VI and vinculin form a molecular apparatus that generates cohesive cell–cell contacts in cultured mammalian epithelia.

## Introduction

Cell–cell contacts are dynamic structures. This is evident during the biogenesis of cultured epithelial monolayers, in which discontinuous early contacts are characteristically replaced by continuous, linear cell–cell adhesions as the epithelia mature (Adams et al., 1998; Vaezi et al., 2002). The maturation of contacts is often accompanied by the appearance of specialized apical epithelial junctions and the establishment of apical–basal polarity (Vaezi et al., 2002). This implies that the transition to coherent linear contacts may represent an important stage in epithelial biogenesis. Cadherin cell adhesion molecules are key features of cellular contacts at all stages of epithelial biogenesis (Adams et al., 1998), and changes in cadherin function are often invoked to account for the dynamic regulation of cell–cell interactions. However, the precise molecular mechanisms responsible for this are not yet thoroughly characterized.

Classic cadherins such as epithelial cadherin (E-cadherin) exert their morphogenetic impact in close cooperation with the actin cytoskeleton (Mege et al., 2006). Actin integrity is essential both for cadherin surface adhesiveness and for cells to make and maintain cadherin-based contacts. Moreover, the capacity of the actin cytoskeleton to support diverse mechanical events, notably surface protrusion, contractility, and anchorage, makes it an ideal partner for cadherin adhesion to mediate dynamic changes at cell–cell contacts. However, the precise molecular mechanisms responsible for this functional interaction are far from clear. Passive scaffolding of cadherin adhesion complexes onto cortical actin filaments, although conceptually simple, has not been empirically verified (Yamada et al., 2005). It is also not evident how any single molecular mechanism for cadherin–actin interactions can readily encompass the diverse functional states that may occur at contacts during epithelial morphogenesis and maturation. Instead, there is increasing evidence that cadherins may interact with a range of different actin effector machinery, including actin nucleators and cross-linkers (Mege et al., 2006).

Actin-based motors are also major determinants of cytoskeletal organization and function. Indeed, to date, three members of the myosin superfamily—myosins II, VII, and VI—have been implicated in cadherin biology. Conventional nonmuscle myosin II has commonly been observed at cell–cell contacts (Dawes-Hoang et al., 2005). Its impact is complex (Ivanov et al., 2005), but, in epithelial cells, myosin II can be recruited and activated in response to E-cadherin ligation, where it serves to promote adhesion and the local accumulation of cadherin at cell–cell contacts (Shewan et al., 2005). Myosin VII was reported to associate indirectly with E-cadherin through the transmembrane

Correspondence to Alpha S. Yap: a.yap@imb.uq.edu.au

Abbreviation used in this paper: DE-cadherin, *Drosophila* E-cadherin; E-cadherin, epithelial cadherin; F-actin, filamentous actin; GAPDH, glyceraldehyde-3-phosphate dehydrogenase; KD, knockdown.

The online version of this article contains supplemental material.


The Journal of Cell Biology, Vol. 178, No. 3, July 30, 2007 529–540
http://www.jcb.org/cgi/doi/10.1083/jcb.200612042

protein vezatin (Kussel-Andermann et al., 2000). Myosin VII is involved in dynamic adhesive events in *Dictyostelium discoideum* (Tuxworth et al., 2001), but its physiological role in mammalian cadherin adhesion remains to be elucidated.

A role for myosin VI in cadherin function was first identified in the egg chamber of *Drosophila melanogaster*. Geisbrecht and Montell (2002) demonstrated that myosin VI was necessary for border cell migration, a morphogenetic process that requires *Drosophila* E-cadherin (DE-cadherin). Moreover, myosin VI and armadillo (*Drosophila* β-catenin) coimmunoprecipitated from ovarian extracts, and myosin VI and DE-cadherin each stabilized the expression of the other protein. Thus, myosin VI and DE-cadherin appeared to be biochemically and functionally interdependent. Myosin VI is unusual among myosins, as it is a minus end–directed motor (Wells et al., 1999; Walker et al., 2000). Accordingly, it has often been thought to participate in vesicle trafficking, both in endocytosis, in which its direction of movement is postulated to promote the internal movement of cargo (Buss et al., 2002; Aschenbrenner et al., 2003; Hasson, 2003), and in exocytosis, especially protein sorting in the biosynthetic pathway (Au et al., 2007). Membrane anchorage coupled with minus end–directed movement may also be a mechanism for myosin VI to exert protrusive force at the cell surface (Geisbrecht and Montell, 2002). However, myosin VI shows limited processivity, and its stepping behavior in vitro is stalled by resistant force, causing it to remain bound to actin filaments for prolonged periods (Altman et al., 2004). Thus, it has been alternatively suggested that myosin VI might act as an actin-based anchor under certain circumstances (Altman et al., 2004). Despite these interesting possibilities, it remains unclear how myosin VI may contribute to the biological activity of DE-cadherin or what its role might be in mammalian cells.

We have now examined the contribution of myosin VI to E-cadherin function in mammalian epithelial cells. We report that myosin VI is recruited to E-cadherin adhesions at a late stage in the maturation of cultured epithelial monolayers. There, it supports cadherin adhesive strength, the morphological integrity of epithelial apical junctions, and the perijunctional actin cytoskeleton.

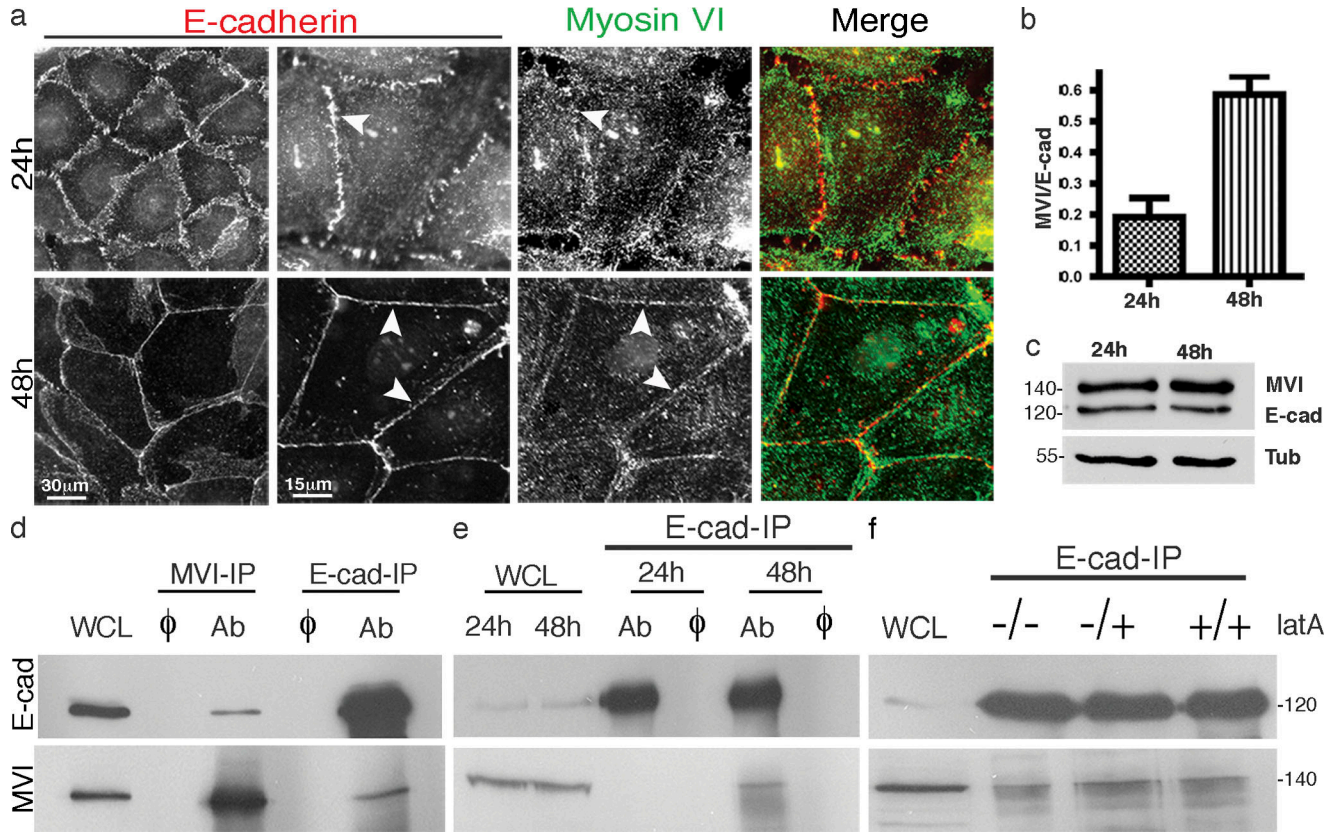


Figure 1. **Myosin VI interacts with E-cadherin as cell–cell contacts mature.** (a) MCF7 cells cultured for 24 or 48 h were immunolabeled for myosin VI and E-cadherin. Myosin VI was readily apparent at E-cadherin contacts (arrowheads) in 48-h-old monolayers but not after 24 h of culture. (b) Ratiometric analysis of myosin VI and E-cadherin fluorescence intensity at cell–cell contacts. Fluorescence intensity of myosin VI staining was expressed as a ratio of E-cadherin fluorescence intensity at the same individual cell–cell contacts. Data are means ± SEM (error bars; $n$ = 30–40 and are representative of four independent experiments). (c) Western blot analysis of myosin VI (MVI) and E-cadherin (E-cad) expression in MCF7 cell lysates. β-Tubulin (Tub) was used as a loading control. (d) Myosin VI coimmunoprecipitates with E-cadherin. Protein complexes were isolated from lysates of 48-h-old MCF7 monolayers using either a myosin VI pAb (MVI-IP) or an anti–E-cadherin pAb (E-cad-IP). Western blots of immunoprecipitates and whole cell lysates (WCL) were probed for E-cadherin or myosin VI. Negative controls for immunoprecipitations were naive rabbit antisera for each corresponding antibody (ϕ). (e) E-cadherin immune complexes were isolated from lysates of MCF7 monolayers after 24 and 48 h of culture and were probed for both E-cadherin and myosin VI. Myosin VI was pulled down with E-cadherin antibody in 48-h-old cultures but not at 24 h despite similar amounts of E-cadherin at each time point. (f) E-cadherin and myosin VI form protein complexes independently of F-actin integrity. E-cadherin immune complexes were isolated from untreated MCF7 cell lysates (−/−), when 100 μM latrunculin A (latA) was added to the lysis buffer (−/+), and from lysates of cells pretreated with 100 μM latrunculin A for 15 min before lysis (as well as having latrunculin included in the lysis buffer; +/+). Western blots were probed for both myosin VI and E-cadherin.

We further demonstrate that myosin VI exerts this effect by recruiting and cooperating with the actin regulator vinculin.

## Results

### Myosin VI preferentially recruits to cohesive E-cadherin–based cell–cell contacts

We began by analyzing the subcellular localization of myosin VI and E-cadherin in MCF7 mammary epithelial cells, which underwent a characteristic morphological transition during culture. 24 h after plating, cells were confluent but displayed E-cadherin staining that was punctate and serrated at the cell–cell contacts, which then became consistently linear and continuous by 48 h (Fig. 1 a). We quantitated this by counting the number of discontinuities in the contacts, which decreased between 24 (14.01 ± 0.81 [±SEM]; $n = 30$) and 48 h (3.00 ± 0.32; $n = 30$). Strikingly, myosin VI was preferentially detected at cell–cell contacts after 48 h, when it coaccumulated with linear E-cadherin (Fig. 1 a, 48 h), whereas relatively little coaccumulated at 24 h. Preferential coaccumulation at these linear (cohesive) contacts was also detected in cells transiently expressing GFP-tagged porcine myosin VI (Fig. S2, available at http://www.jcb.org/cgi/content/full/jcb.200612042/DC1). Similarly, in MDCK monolayers, myosin VI became detectable only when cells formed extensive, continuous contacts (unpublished data), although this process was more rapid than in MCF7 cells.

The preferential localization of myosin VI in older, cohesive contacts was not caused by changes in the total cellular expression of this protein (Fig. 1 c), nor did it simply reflect increased local amounts of E-cadherin at contacts. Although fluorescence intensity at contacts of both E-cadherin and myosin VI increased with time (Fig. S3 a, available at http://www.jcb.org/cgi/content/full/jcb.200612042/DC1), ratiometric analysis revealed that 48-h-old cultures possessed substantially more myosin VI at contacts relative to E-cadherin than did 24-h-old cultures (Fig. 1 b). Therefore, the comparatively late recruitment of myosin VI to cadherin contacts occurred independently of changes in the levels of E-cadherin at those contacts.

We then used coimmunoprecipitation analysis to test whether myosin VI formed a biochemical complex with E-cadherin. Myosin VI was detected in E-cadherin immunoprecipitates, and E-cadherin was identified in myosin VI immune complexes (Fig. 1 d), confirming a previous study of *Drosophila* (Geisbrecht and Montell, 2002). This interaction persisted when actin filament integrity was disrupted by 100 μM latrunculin A (Fig. 1 f). Moreover, a biochemical complex between these two proteins was only detected after 48 h of culture, which is coincident with the appearance of myosin VI at cadherin contacts (Fig. 1 e). In contrast, Mena and WAVE, which are other actin regulators found at cell–cell contacts (Scott et al., 2006; Yamazaki et al., 2007), did not coimmunoprecipitate with E-cadherin (unpublished data). These findings indicate that myosin VI is preferentially recruited

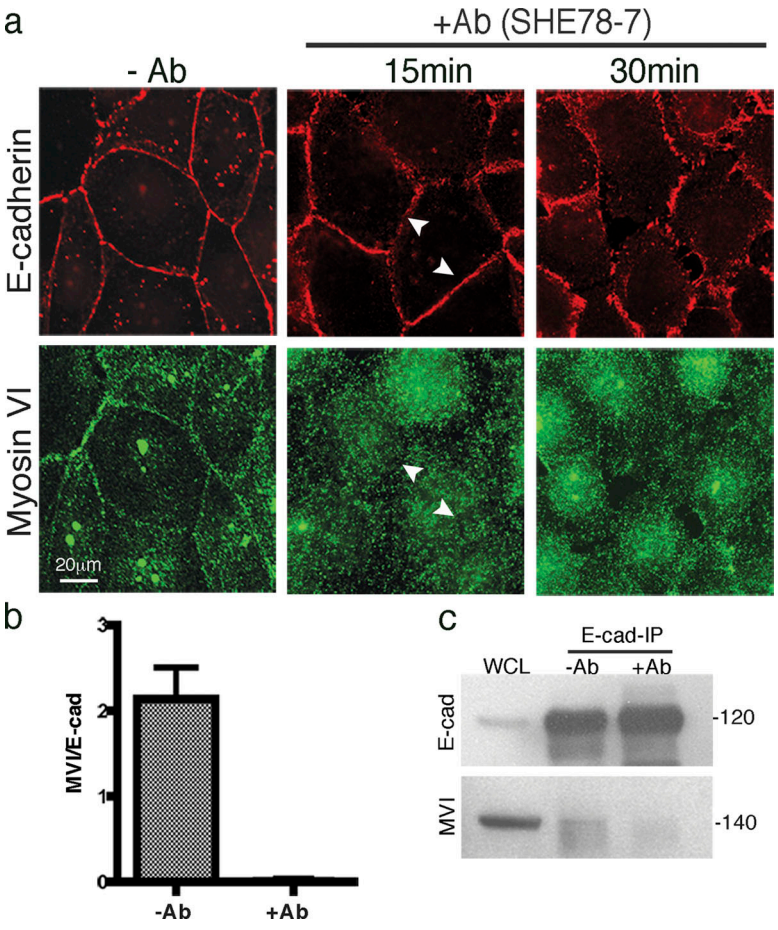


Figure 2. **E-cadherin adhesion is necessary to recruit myosin VI to cell–cell contacts.** (a) 48-h-old MCF7 cell monolayers were incubated in medium alone (−Ab) or in the presence of the E-cadherin function-blocking mAb SHE78-7 for 15–30 min. E-cadherin was detected using a mouse mAb against the cytoplasmic domain, whereas myosin VI was detected using myosin VI pAb. SHE78-7 abolished myosin VI staining at cadherin contacts within 15 min, before the integrity of the contacts was overtly disrupted (arrowheads). (b) Ratiometric analysis of myosin VI (MVI)/E-cadherin fluorescence intensity at cell–cell contacts in control cultures (−Ab) and cultures treated with SHE78-7 for 15 min (+Ab). Data are means ± SEM (error bars; $n = 30–40$ and are representative of four independent experiments). (c) E-cadherin immune complexes isolated from control monolayers (−Ab) or monolayers treated with SHE78-7 for 30 min (+Ab) were probed for myosin VI and E-cadherin.

into E-cadherin complexes as cells form linear, cohesive contacts with one another.

### Recruitment of myosin VI to cell–cell contacts requires E-cadherin function

To test whether E-cadherin adhesion was responsible for recruiting myosin VI to cellular contacts, we treated 48-h-old MCF7 monolayers with a function-blocking anti–E-cadherin antibody (SHE78-7). As shown in Fig. 2 a, myosin VI staining was displaced from cell–cell contacts as early as 15 min after exposure to the antibody, before the integrity of the cell–cell contacts was overtly disrupted. This was confirmed by the measurement of myosin VI and E-cadherin fluorescence, which showed that myosin VI intensity fell rapidly relative to E-cadherin staining in cells treated with SHE78-7 antibody (Figs. 2 b and S3 b). Consistent with these immunofluorescence results, less myosin VI coimmunoprecipitated with E-cadherin 30 min after the addition of SHE78-7 antibody (Fig. 2 c). Together, these findings demonstrated that productive adhesion was necessary for E-cadherin to recruit myosin VI.

### Myosin VI depletion disrupts cell adhesion and junctional integrity at cell–cell contacts

We then used RNAi to test the functional impact of myosin VI on E-cadherin. Two different siRNAs consistently reduced myosin VI expression by 80–100% for up to 7 d (Fig. 3 a). Because these

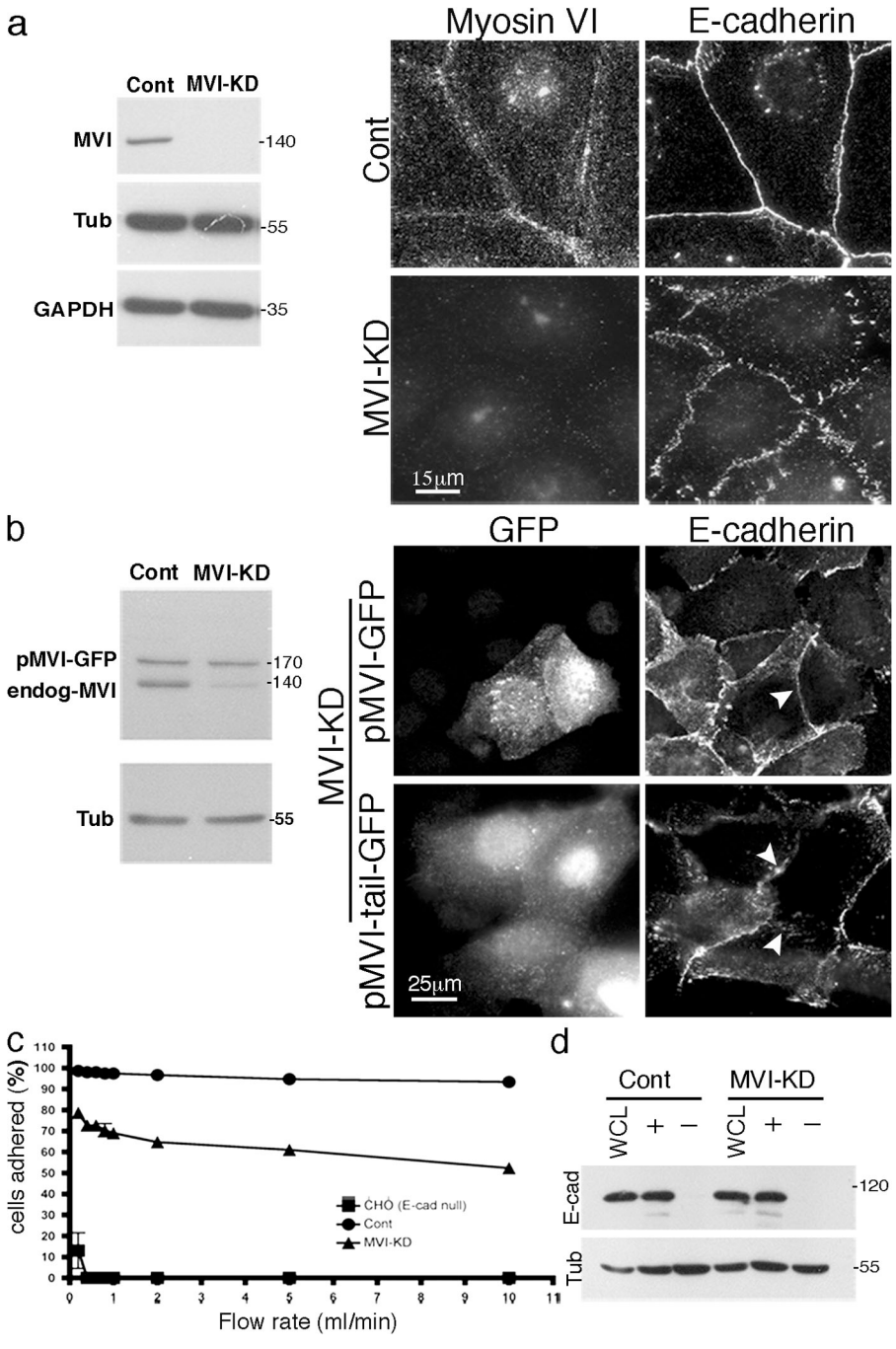


Figure 3. **Myosin VI is necessary for E-cadherin adhesion and cohesive cell–cell contacts.** MCF7 cells were transiently transfected with siRNA directed against human myosin VI (MVI-KD) or with control duplexes bearing a single mismatched base pair (Cont). (a) siRNA depletes myosin VI. Western analysis of myosin VI expression in cells 6 d after transfection. Loading controls were β-tubulin (Tub) and GAPDH. Indirect immunofluorescence microscopy showed that myosin VI was largely undetectable at E-cadherin contacts. Compared with control cells, E-cadherin staining in myosin VI KD cells was punctate and discontinuous. (b) Exogenous myosin VI rescues cell contact integrity in myosin VI KD cells. Myosin VI expression was reconstituted by the transient expression of porcine myosin VI tagged with EGFP (pMVI-GFP). Western blotting for myosin VI revealed both the transgene and endogenous myosin VI. Endogenous human myosin VI expression was reduced, but that of the transgene was not affected by the myosin VI siRNA. Linear, continuous E-cadherin staining was seen at contacts between cells expressing pMVI-GFP (arrowhead) compared with untransfected controls or cells expressing the myosin VI tail domain alone (pMVI–tail-GFP; arrowheads). (c) Depletion of myosin VI reduces E-cadherin–based adhesion. Adhesion of control MCF7 cells or myosin VI KD cells to hE/Fc-coated substrata was measured using laminar flow assays and was expressed as the percentage of cells that remained adherent to hE/Fc at various detachment flow rates. E-cadherin–deficient CHO cells were used as negative controls. Data are means ± SEM (error bars; $n = 3$) and are representative of four independent experiments. (d) Myosin VI KD does not affect the total or surface expression levels of E-cadherin. Surface expression of E-cadherin was measured using surface trypsin protection assays in control cells or in cells depleted of myosin VI. Cells were lysed before (WCL) or after trypsinization in the presence (+) or absence (−) of extracellular $Ca^{2+}$. Total levels of E-cadherin were unaffected by myosin VI KD, and surface E-cadherin remained sensitive to trypsinization in the absence of $Ca^{2+}$ (−) in both the control and myosin VI–depleted cells. β-Tubulin was the loading control.

duplexes yielded similar effects, data are only shown for one siRNA. Myosin VI protein expression was not affected by either scrambled oligonucleotides or a control duplex (Fig. 3 a, Cont) bearing a single nucleotide mismatch from the knockdown (KD) sequence, nor were β-tubulin or glyceraldehyde-3-phosphate dehydrogenase (GAPDH) levels affected by the siRNA (Fig. 3 a).

Depletion of myosin VI dramatically altered the morphology of cell–cell contacts. Whereas control cultures retained E-cadherin with a continuous linear distribution at the contacts, myosin VI KD cells showed punctate and serrated E-cadherin staining (Fig. 3 a) similar to that seen in 24-h-old control cultures before the appearance of myosin VI (Fig. 1). Quantitation confirmed an increased number of discontinuities in contacts from myosin VI KD cells ($14.50 \pm 0.77$; $n = 30$) compared with control cells ($2.60 \pm 0.34$; $n = 30$). Similarly, the transient expression of a dominant-negative myosin VI mutant lacking the motor head domain (p–myosin VI–tail-GFP) markedly disrupted cell morphology and cell–cell contacts (unpublished data). This suggested that myosin VI might critically influence the morphological transition of cell–cell contacts over time.

Consistent with this, the reconstitution of myosin VI using porcine myosin VI (p–myosin VI–GFP), which is resistant to KD (Fig. 3 b), rescued the phenotype of myosin VI KD cells. Myosin VI KD cells expressing p–myosin VI–GFP regained linear E-cadherin staining at their cell–cell contacts compared with the punctate E-cadherin distribution of untransfected neighboring cells (Fig. 3 b). However, the transient expression of p–myosin VI–tail-GFP failed to rescue the myosin VI KD phenotype (Fig. 3 b), indicating that the actin-binding motor head was necessary for myosin VI to affect junctional maturation.

We then directly tested the adhesive impact of myosin VI using laminar flow adhesion assays that measure the cellular resistance to detachment from substrata coated with recombinant cadherin ligand (hE/Fc). Myosin VI KD resulted in an ~40% reduction in adhesive strength compared with cells transfected with control duplexes (Fig. 3 c). In contrast, integrin-based

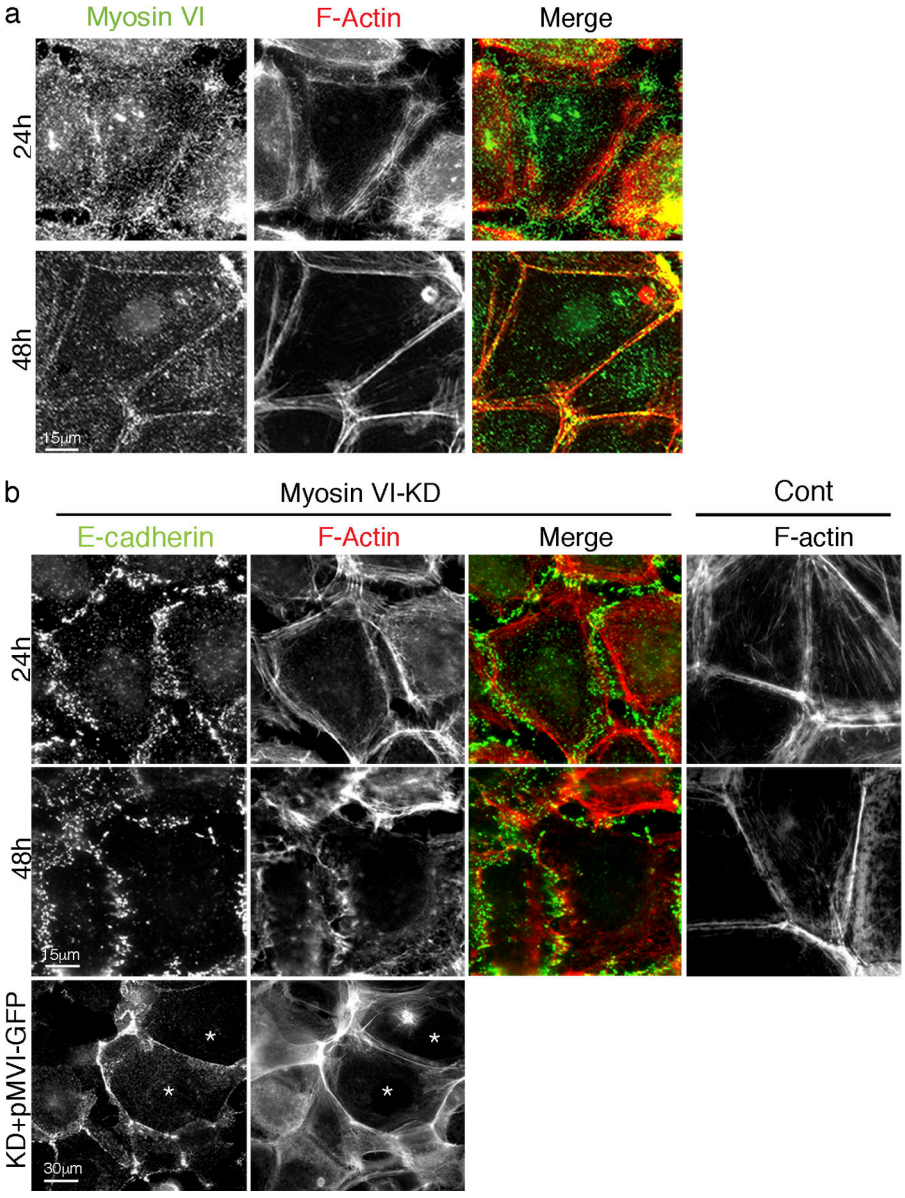


Figure 4. **Myosin VI affects the perijunctional actin cytoskeleton.** (a) Reorganization of the perijunctional actin cytoskeleton coincides with the accumulation of myosin VI. MCF7 cells cultured for 24 or 48 h were labeled for F-actin (phalloidin) and myosin VI. Whereas 24-h-old cultures showed loose perijunctional phalloidin staining, F-actin accumulated intensely at the cell–cell contacts in 48-h-old cultures. (b) Myosin VI depletion disrupts organization of the perijunctional actin cytoskeleton in 24- and 48-h-old cultures. Myosin VI KD cells showed loose perijunctional phalloidin staining compared with the dense peripheral staining seen in control (Cont) cells. E-cadherin was used to identify the cell–cell contacts between myosin VI KD cells. The dense perijunctional F-actin staining was restored in cells transiently expressing porcine myosin VI (KD + pMVI-GFP; asterisks).

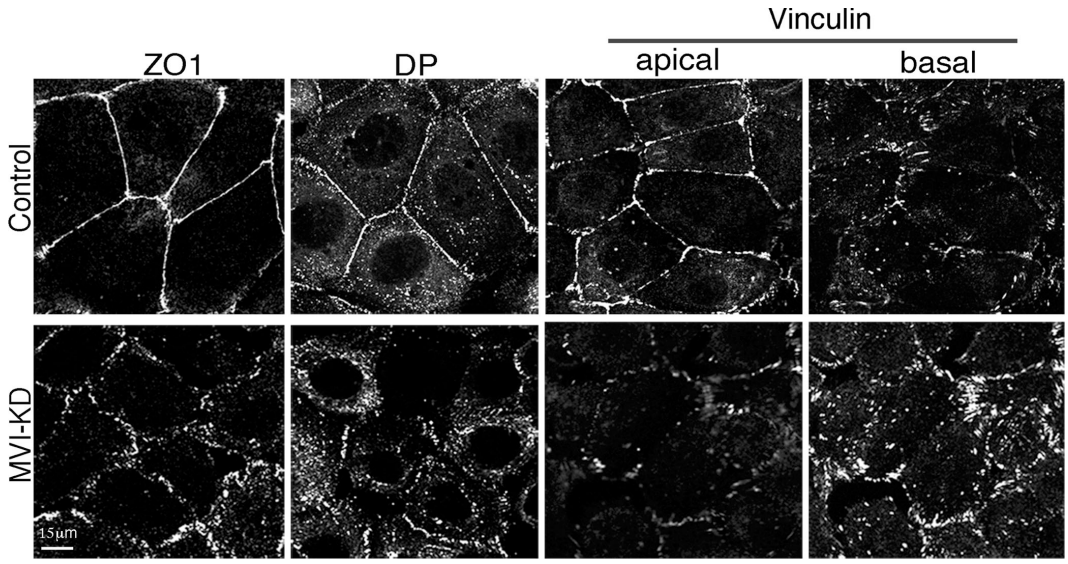


Figure 5. **Myosin VI supports the integrity of apical junctional complexes.** Myosin VI KD and control MCF7 monolayers were immunolabeled for ZO-1, desmoplakin (DP), or vinculin to identify tight junctions, desmosomes, and the zonula adherens, respectively, and were imaged by spinning disc confocal microscopy. Vinculin was nearly totally lost from the apical cell–cell contacts in myosin VI KD cells, whereas vinculin staining in basal focal adhesions persisted.

adhesion to fibronectin was unaffected by myosin VI depletion (Fig. S4, available at http://www.jcb.org/cgi/ content/full/jcb .200612042/DC1), suggesting that myosin VI preferentially affected cadherin adhesion. Myosin VI KD did not affect the total or surface levels of E-cadherin (Fig. 3 d and Fig. S5, a and c), the cellular expression of catenins, or their binding to E-cadherin (Fig. S5, a and b).

### Myosin VI affects actin organization in epithelial monolayers

Filamentous actin (F-actin), like E-cadherin, undergoes a distinct morphological transition as epithelial monolayers mature in culture. After 24 h, F-actin staining appeared relatively loosely organized in the perijunctional regions, whereas by 48 h, F-actin was densely accumulated at the cell–cell contacts (Fig. 4 a). This dense actin organization was lost in KD cells but not in control cells, most evidently at 48 h (Fig. 4 b). Expression of porcine myosin VI restored the dense perijunctional F-actin staining (Fig. 4 b). Interestingly, the total cellular levels of F-actin were not altered in KD cells (unpublished data), suggesting that myosin VI regulates the perijunctional organization of F-actin rather than affecting the global actin filament content of the cells.

### Myosin VI supports the integrity of the epithelial apical junctional complex

E-cadherin adhesion is necessary for biogenesis of the specialized intercellular structures that comprise the apical junctional complex of epithelia (Gumbiner et al., 1988). Therefore, we next examined the impact of myosin VI depletion on the integrity of the junctional complex (Fig. 5). In control MCF7 monolayers, the tight junction marker ZO-1 displayed crisp, linear immunofluorescent staining throughout the apical-most regions of cell–cell contacts. In contrast, ZO-1 staining was discontinuous and fragmented in myosin VI KD monolayers. Similarly, staining for the desmosomal marker desmoplakin was distributed unevenly at contacts between myosin VI KD cells but was homogenous throughout contacts between control cells. However, despite this fragmentation, both ZO-1 and desmoplakin showed persistent staining in regions of contacts that retained E-cadherin (unpublished data), suggesting that the disruption of both tight junctions and desmosomes might reflect the loss of cohesive integrity between the cells.

In contrast, staining for vinculin, a marker of the zonula adherens (Geiger et al., 1980), was nearly completely lost from cell–cell contacts in myosin VI KD cells, even where E-cadherin persisted (Fig. 5). Vinculin also marks focal adhesions, but myosin VI depletion did not displace vinculin from these cell–matrix adhesive junctions, which is consistent with our observation that integrin-based adhesion was unaffected by myosin VI KD. Total cellular levels of vinculin were also not affected by myosin VI KD (Fig. S5 a), implying that myosin VI regulated the recruitment of vinculin to cadherin adhesions. As vinculin is reported to interact with the E-cadherin complex (Watabe-Uchida et al., 1998; Weiss et al., 1998), we investigated whether myosin VI participated in this biochemical interaction. Indeed, coimmunoprecipitation analysis identified an apparent complex containing E-cadherin, vinculin, and myosin VI in 48-h-old control MCF7 cells. Immune complexes generated with antibodies to any of these three proteins also contained the other two proteins (Fig. 6 a). However, the ability of vinculin to coimmunoprecipitate with E-cadherin was lost in myosin VI KD cells (Fig. 6 b). Therefore, myosin VI was necessary for vinculin to stably interact with E-cadherin in mature cell–cell contacts. The ability to bind both vinculin and E-cadherin resides in the myosin VI tail, as transiently expressed p–myosin VI–tail-GFP was able to coimmunoprecipitate these proteins (Fig. 6 c). Moreover, cross-linking by actin filaments cannot

readily account for this interaction, as this myosin VI fragment lacks the actin-binding head domain.

### Vinculin is a downstream effector of myosin VI at cell–cell contacts

Interestingly, vinculin-deficient F9 embryonal carcinoma cells were reported to show defects in cell–cell cohesion reminiscent of those we observed upon the depletion of myosin VI (Watabe-Uchida et al., 1998). This led us to postulate that vinculin might be responsible for the impact of myosin VI on cell–cell integrity. To test this, we first examined the impact of depleting vinculin itself (Fig. 7). siRNA effectively reduced cellular vinculin levels (Fig. 7 a), most comprehensively at cell–cell contacts (not depicted). Importantly, junctional continuity was disrupted by vinculin KD (Fig. 7 b), with E-cadherin staining becoming punctate and serrated (14.40 ± 0.81 discontinuities/contact; $n = 30$) compared with control transfections (2.77 ± 0.45 discontinuities/contact; $n = 30$). Thus, the impact of vinculin KD on E-cadherin organization resembled that of myosin VI KD. However, neither myosin VI levels (Fig. S5 d) nor the ability of myosin VI to coimmunoprecipitate with E-cadherin were affected in vinculin KD cells (Fig. 7 c), nor were total cellular levels of E-cadherin or catenins perturbed by vinculin KD (Fig. S5 d).

Then, we asked whether the restoration of vinculin activity might affect the myosin VI KD phenotype (Fig. 8). Because full-length vinculin readily adopts an autoinhibited conformation (Johnson and Craig, 1995), we used membrane-directed fragments of vinculin that restored tight junction integrity in F9 cells (Watabe-Uchida et al., 1998). We transiently expressed chimeric constructs bearing the head (α-cat/vinHead) or tail (α-cat/vinTail) region of vinculin (Fig. 8 a) fused to the β-catenin–binding domain of α-catenin to target them to cadherin contacts and not to focal adhesions. Both proteins consistently localized to cell–cell contacts (Fig. 8 b). Strikingly, we found that both of these transgenes also restored the continuous linear organization of E-cadherin at contacts between myosin VI KD cells (Fig. 8, b and c). The α-cat/vinHead construct rescued contact integrity somewhat more efficiently than did the α-cat/vinTail construct, but both rescued much more effectively than did full-length α-catenin alone (Fig. 8, b and c).

Furthermore, we reasoned that if vinculin acts downstream of myosin VI, vinculin would be necessary for myosin VI to support the cohesive integrity of cell–cell contacts. As KD and reconstitution provides a strategy to isolate the activity of a specific protein, we tested whether exogenous myosin VI could rescue E-cadherin organization when vinculin as well as endogenous myosin VI were depleted (Fig. 9 a). Importantly, the transient expression of porcine myosin VI–GFP was unable to rescue linear cadherin contacts in double vinculin/myosin VI KD cells (Fig. 9, a and c). This indicated that vinculin was necessary for the reconstitution of myosin VI to be effective. Finally, we tested whether myosin VI could compensate for the loss of vinculin and found that the overexpression of myosin VI did not restore the integrity of contacts in vinculin single KD cells (Fig. 9, b and c). Together, these findings identify vinculin as a critical effector for myosin VI at cohesive cell–cell contacts.

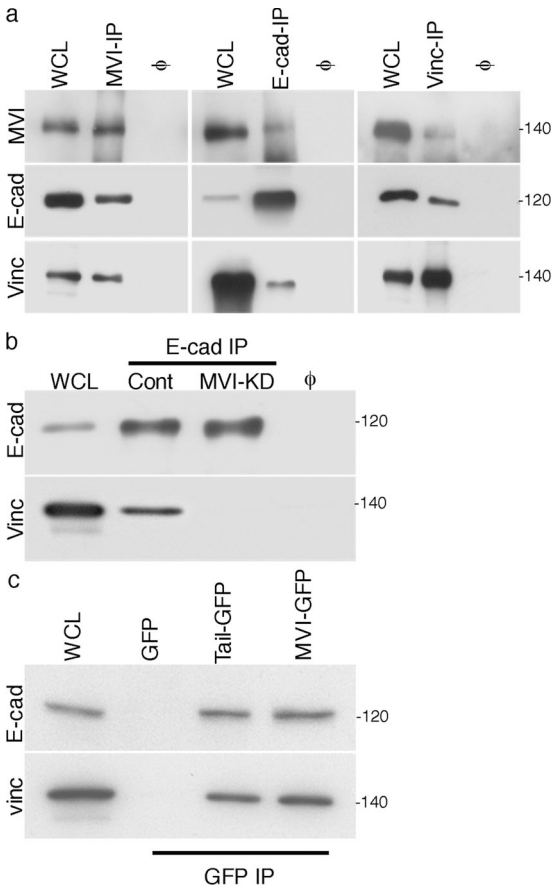


Figure 6. **Myosin VI is necessary for E-cadherin and vinculin to interact.** (a) Myosin VI, E-cadherin, and vinculin are found in a complex. Protein complexes were immunoprecipitated from 48-h-old MCF7 monolayers using either a myosin VI pAb (MVI-IP), E-cadherin pAb (E-cad-IP), or vinculin mAb (Vinc-IP). Western blots of immunoprecipitates and whole cell lysates (WCL) were probed for E-cadherin, myosin VI, and vinculin. Negative controls for immunoprecipitations were naive rabbit antisera for E-cadherin and myosin VI and anti-HA monoclonal antibody for vinculin (ϕ). (b) E-cadherin is unable to immunoprecipitate vinculin in the absence of myosin VI. Western blots of E-cadherin immunoprecipitates (E-cad IP) and whole cell lysates (WCL) from myosin VI KD or control cells were probed for E-cadherin or vinculin. Negative controls for immunoprecipitations (ϕ) were naive rabbit antisera. (c) The myosin VI tail coimmunoprecipitates E-cadherin and vinculin. Full-length p–myosin VI–GFP, p–myosin VI–tail-GFP, and GFP alone were transiently expressed in MCF7 cells. Western blots of anti-GFP immune complexes were probed for E-cadherin and vinculin. Blotting for GFP (on separate gels because of the disparate molecular weights) confirmed that the transgenes expressed polypeptides of predicted molecular weight and were immunoprecipitated to a similar level (not depicted).

## Discussion

Cadherin-based cell–cell contacts undergo distinct morphological transitions both in vivo and in vitro, even after cells have established contact with one another. The challenge is to define specific molecular mechanisms responsible for the morphogenesis of these cell–cell interactions. Our current work identifies myosin VI as an important factor that interacts with cadherin adhesion to control the process by which early discontinuous interactions become organized into cohesive, linear contacts as epithelial monolayers mature in culture. We found that myosin VI binds to E-cadherin and localizes at cell–cell contacts as they undergo the transition from discontinous to coherent

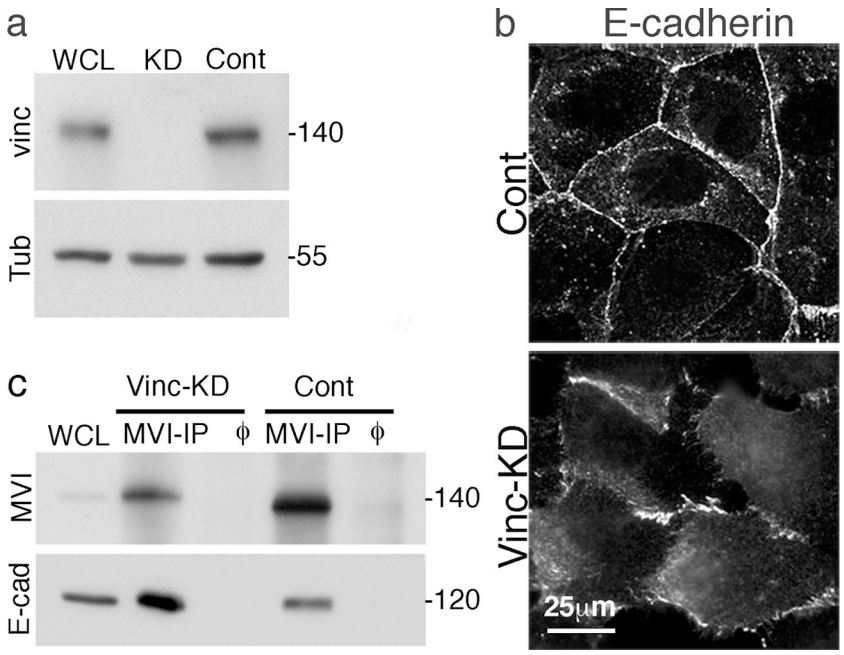


Figure 7. **Vinculin depletion disrupts the integrity of E-cadherin cell–cell contacts.** MCF7 cells were transiently transfected with siRNA duplexes against human vinculin (Vinc-KD) or a control duplex with a 4-bp substitution (Cont). (a) Immunoblotting for vinculin and tubulin confirmed the efficient depletion of vinculin. (b) Immunofluorescence staining revealed that E-cadherin cell–cell contacts were discontinuous and serrated in vinculin KD cells compared with controls. (c) Vinculin is not necessary for myosin VI to coimmunoprecipitate E-cadherin. Myosin VI was immunoprecipitated from vinculin-depleted (Vinc-KD) or control cultures and immune complexes probed for both myosin VI and E-cadherin. Negative controls for immunoprecipitations were naive rabbit antisera (ϕ).

and continuous. This appears to reflect a regulated recruitment process, as cellular levels of myosin VI do not change during this period. Importantly, the disruption of myosin VI function by RNAi or expression of a dominant-negative mutant perturbed the cohesive integrity of cell–cell contacts and reduced cadherin adhesion. Moreover, myosin VI depletion perturbed the integrity of tight junctions and desmosomes, which is consistent with the central role for E-cadherin function in junctional biogenesis (Gumbiner et al., 1988). In contrast, myosin VI had no effect on integrin-based cell adhesion to fibronectin. Thus, in cultured mammalian cells, myosin VI acts at a relatively late stage in epithelial maturation to generate cohesive cell–cell interactions.

Our findings support and extend earlier evidence from *Drosophila* that implicated myosin VI in cadherin-based cell–cell interactions. Myosin VI cooperates with DE-cadherin to support morphogenetic movement in the fly egg chamber (Geisbrecht and Montell, 2002). Specifically, myosin VI is expressed and forms a complex with DE-cadherin and armadillo in migrating border cells. Importantly, myosin VI is necessary for this cadherin-dependent form of cell-on-cell migration, which is consistent with our finding that myosin VI supports cadherin adhesion and aspects of cellular morphogenesis in mammalian epithelia. Similarly, the disruption of myosin VI perturbed intercellular cohesion, DE-cadherin localization, and dorsal closure during early fly morphogenesis (Millo et al., 2004). Collectively, our findings in mammalian cells, taken with these earlier precedents in invertebrates, suggest an important conserved contribution of myosin VI to cadherin function.

How might myosin VI regulate cadherin contacts and adhesion in mammalian epithelia? This unconventional motor has been implicated in two broad cellular processes: membrane transport and actin filament organization. Myosin VI is recruited to clathrin-coated pits and persists on the subsequent uncoated vesicles, likely through interaction with several adaptor proteins (Buss et al., 2001; Aschenbrenner et al., 2003). This, taken with its minus end–directed movement, has suggested a role in endocytosis (Buss et al., 2002). Myosin VI also associates with the Golgi apparatus and can support exocytotic transport (Warner et al., 2003). Indeed, in MDCK cells, myosin VI was necessary for the basolateral delivery of proteins that contain tyrosine-based motifs sorted by the AP-1B clathrin adaptor complex (Au et al., 2007). However, myosin VI did not affect protein sorting that depended on dileucine motifs, including E-cadherin (Bryant and Stow, 2004). Similarly, we found no substantial change in either the total or surface levels of E-cadherin in myosin VI KD cells, nor could we detect changes in the transport of E-cadherin to the cell surface (unpublished data). Thus, although myosin VI may play a more subtle role in cadherin trafficking, this pathway does not readily account for our results.

Instead, we favor the notion that myosin VI participates in cadherin–actin cooperation. We found that the perijunctional actin cytoskeleton was clearly disrupted by myosin VI depletion. As epithelial monolayers matured, reorganization of the perijunctional actin cytoskeleton accompanied the appearance of linear, cohesive cadherin contacts, an initially loose distribution of F-actin being replaced by dense staining concentrated in the immediate vicinity of cell–cell contacts. In myosin VI KD cells, the dense perijunctional packing of F-actin was replaced by a looser organization, without any concomitant change in total cellular F-actin levels. Similarly, earlier studies reported that myosin VI can stabilize actin filament networks (Noguchi et al., 2006) and potentially filaments themselves (Naccache and Hasson, 2006), characteristically promoting the dense packing and accumulation of filaments. For example, during spermatid individualization in *Drosophila*, myosin VI is necessary to organize the actin cones that separate the syncytial spermatids. Notably, the density of filaments in the actin cones is substantially reduced in myosin VI mutant testes without apparent changes in filament turnover, suggesting that myosin VI participates in packing and

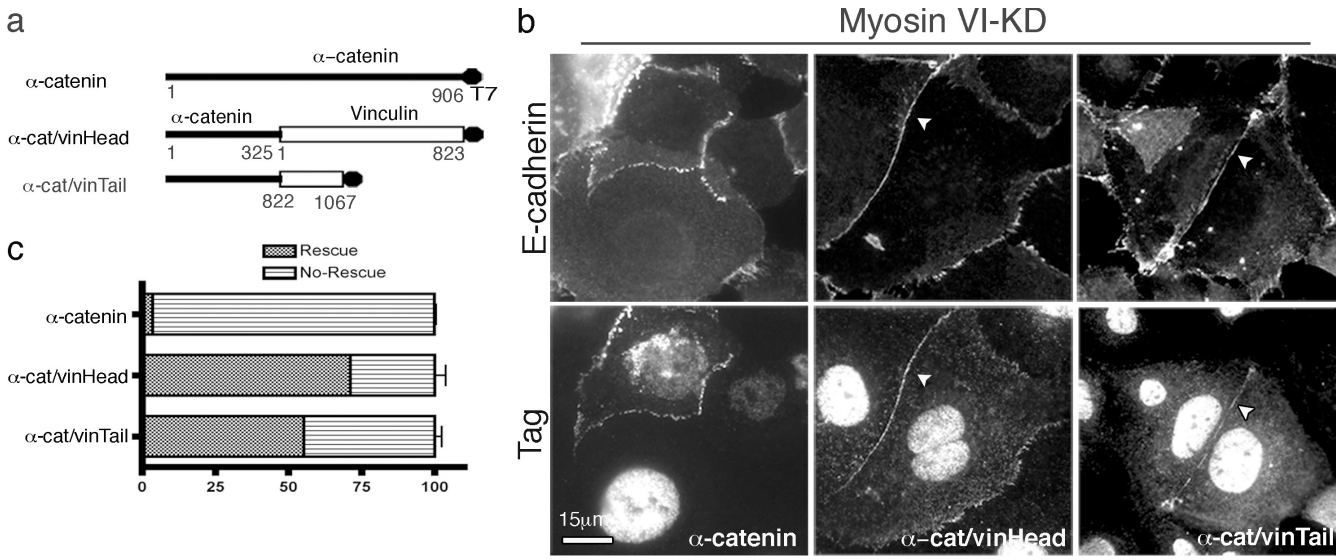


Figure 8. **Membrane-targeted vinculin fragments rescue cell–cell integrity in myosin VI–depleted cells.** (a) Schematic of constructs: full-length αE-catenin bearing a C-terminal T7 tag (α-catenin) and α-catenin/vinculin chimeric proteins in which the N-terminal 1–325 amino acid domain of α-catenin was fused to the N-terminal 1–823 head domain of vinculin (α-cat/vinHead) or the C-terminal 822–1,067 tail domain of vinculin (α-cat/vinTail). (b) Expression of vinculin constructs but not α-catenin rescues the integrity of E-cadherin cell–cell contacts in myosin VI–depleted cells. Myosin VI KD cells were transiently transfected with α-catenin–vinculin constructs or full-length α-catenin and were fixed and stained for E-cadherin. Transfected cells were identified by the T7 tag; nuclear staining in the T7-stained cells is background, as it was detected in nontransfected controls (not depicted). Linear E-cadherin contacts were frequently restored in cells expressing either α-catenin/vinculin construct (arrowheads). (c) Quantitation revealed that α-cat/vinTail did not rescue as frequently as αE/vinHead, whereas α-catenin was unable to rescue E-cadherin contact integrity to any comparable extent. Data are means ± SEM (error bars; $n = 100$ and are representative of five independent experiments).

organizing actin filament networks (Noguchi et al., 2006). The impact of myosin VI on organization of the perijunctional actin cytoskeleton implies that a similar contribution may occur in epithelial cells.

Importantly, several lines of evidence identify the actin-binding protein vinculin as a downstream effector for myosin VI at cadherin adhesions. (1) Myosin VI was necessary for vinculin to stably associate with E-cadherin in mature epithelial monolayers, which was assessed by both coimmunoprecipitation and immunofluorescence analysis. Vinculin was also selectively lost from cell–cell contacts but not focal adhesions in myosin VI KD cells. However, the ability of myosin VI to interact with E-cadherin was not affected by vinculin KD, implying that vinculin recruitment to E-cadherin is downstream of myosin VI. (2) Vinculin KD disrupted the integrity of cohesive E-cadherin contacts in a manner similar to myosin VI KD. (3) Membrane-targeted vinculin fragments effectively restored the cohesive integrity of cadherin contacts in myosin VI KD cells. This implied that reconstitution of vinculin function at E-cadherin adhesions could compensate for the global loss of myosin VI. (4) Vinculin was necessary for myosin VI to regulate junctional integrity. Exogenous myosin VI could not rescue contact integrity in cells depleted of vinculin as well as endogenous myosin VI, indicating that vinculin was necessary for the reconstitution of myosin VI to be effective. (5) Myosin VI could not compensate for the loss of vinculin, as the overexpression of myosin VI did not rescue contact integrity in vinculin KD cells. This argues against the possibility that vinculin and myosin VI are in parallel pathways. Collectively, these findings indicate that vinculin is an important effector for myosin VI at cadherin contacts.

Vinculin has long been recognized to accumulate at cell–cell contacts, where it is thought to incorporate into adherens junctions (Geiger et al., 1980). However, it is notable that previous studies implicated α-catenin in recruiting vinculin to cadherin adhesions (Watabe-Uchida et al., 1998; Weiss et al., 1998). We, too, found that vinculin stains in early cell–cell contacts (unpublished data) before myosin VI is readily detected, a process that therefore may entail α-catenin. Yet, in our experience, myosin VI was necessary for vinculin to stably incorporate into mature cadherin adhesions. This suggests that two mechanisms participate in localizing vinculin to cadherin adhesions, with myosin VI being dominant at a later stage than α-catenin.

Thus, our findings identify myosin VI and vinculin as part of a molecular apparatus responsible for generating the cohesive cell–cell contacts that distinguish epithelial biogenesis in vitro. We postulate that myosin VI and vinculin cooperate to reorganize the perijunctional actin cytoskeleton, leading to the generation of cohesive, linear cadherin contacts. Precisely how vinculin participates in this process has yet to be defined at a molecular level. Vinculin can both bind and bundle actin filaments (Jockusch and Isenberg, 1981; Menkel et al., 1994; Huttelmaier et al., 1997; Janssen et al., 2006), so may provide a mechanism to organize and compact actin filament meshworks at cadherin adhesions. The actin-binding site has been mapped to the tail region of the vinculin molecule (Johnson and Craig, 2000). Therefore, it was interesting to note that the head fragment could also rescue contact integrity. The mechanism for this effect remains to be determined.

However, our data further indicate that myosin VI does not act only by recruiting vinculin into a cadherin-based complex. Although the myosin VI tail alone can coimmunoprecipitate both

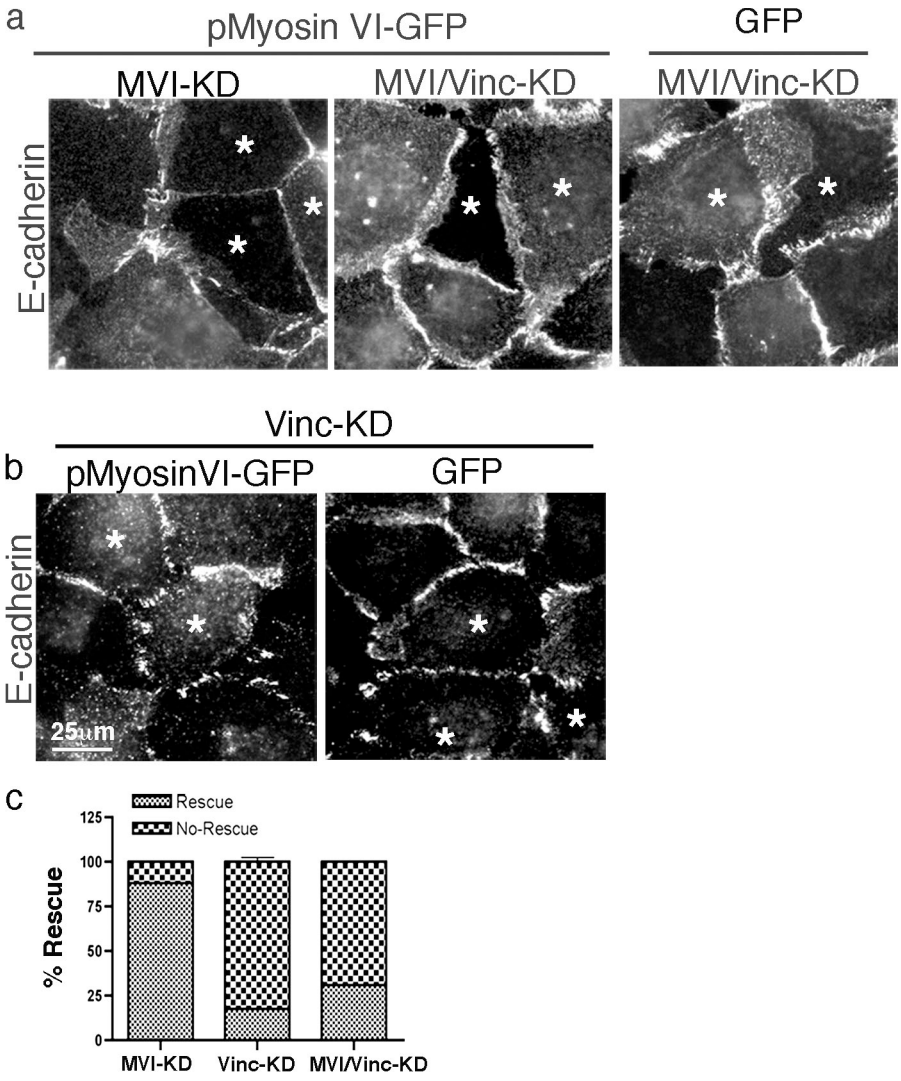


Figure 9. **Vinculin is necessary for myosin VI to regulate cadherin contacts.** (a) Myosin VI reconstitution requires vinculin to restore the integrity of E-cadherin contacts. Porcine myosin VI (p–myosin VI–GFP) or GFP alone (GFP) were transiently expressed in MCF7 cells transfected with siRNA for myosin VI alone (MVI-KD) or with siRNA for both myosin VI and vinculin (MVI/Vinc-KD). Cells were stained for E-cadherin and the GFP tag; cells expressing p–myosin VI–GFP or GFP are denoted by asterisks. P–myosin VI–GFP failed to restore linear cadherin contacts in myosin VI/vinculin double KD cells. (b) Overexpression of myosin VI does not rescue linear cadherin contacts in vinculin-depleted cells. P–myosin VI–GFP or GFP alone were transiently expressed in cells transfected with siRNA for vinculin. Samples were stained for E-cadherin, and cells expressing the transgene (asterisks) were identified by GFP. (c) Rescue of linear contacts by myosin VI. The ability of p–myosin VI–GFP to rescue linear cadherin contacts was assessed in cells depleted of myosin VI alone (MVI-KD), vinculin alone (Vinc-KD), and depleted of both myosin VI and vinculin (MVI/Vinc-KD). Contacts were scored based on whether they were linear (rescue) or discontinuous (no rescue); data are means ± SEM (error bars; $n = 100$ and are representative of five independent experiments).

E-cadherin and vinculin and localize to cell–cell contacts (unpublished data), this fragment did not rescue the cohesive integrity of those contacts in myosin VI KD cells. Therefore, the actin-binding activity of the myosin VI head domain must functionally cooperate with vinculin for myosin VI to support cohesive cell–cell contacts. The nature of this cooperation remains to be determined. Our data do not exclude the possibility that other proteins participate in this myosin VI–based effector pathway. One speculative possibility is that myosin VI may serve as an actin-based anchor (Altman et al., 2004), cooperating with vinculin's ability to organize actin in order to link cadherin complexes onto perijunctional actin filaments. Perhaps this cooperative interaction with actin also serves to stabilize vinculin at contacts, accounting for the role of myosin VI to stably localize vinculin in mature contacts.

Irrespective of the deep molecular mechanism, our findings highlight the concept that multiple actin regulators operate at cadherin adhesive contacts, and they reinforce the notion that the functional expression of individual mechanisms is likely to be tightly regulated by cellular context. Understanding the regulated recruitment of myosin VI will be important if we are to elucidate the varied molecular mechanisms that cadherin adhesion uses to regulate the actin cytoskeleton.

## Materials and methods

### Cell culture, transfections, hE/Fc, and adhesion assays

MCF-7 cells and CHO cells have been described previously (Goodwin et al., 2003; Helwani et al., 2004). For transient expression, cells were transfected with LipofectAMINE 2000 (Invitrogen) according to the manufacturer's instructions and analyzed 24–48 h after transfection. hE/Fc was prepared and used as previously described (Kovacs et al., 2002).

hE/Fc-based laminar flow adhesion assays were performed as described previously (Verma et al., 2004). Integrin-based adhesion assays were performed using longer term adhesion assays (Verma et al., 2004) with alterations to substrata coating. In brief, poly-L-lysine–coated six-well plates were incubated overnight at 4°C with 10 μg/ml fibronectin (Sigma-Aldrich) in PBS and were incubated with HBSS containing 5 mM $CaCl_2$ for 30 min at 37°C. Cells were isolated by incubation for 10 min in 0.01% (wt/vol) crystalline trypsin (Sigma-Aldrich) in HBSS containing 5 mM $CaCl_2$. Freshly isolated cells were allowed to attach to substrata for 90 min at 37°C in a $CO_2$ incubator and were subjected to detachment by systematic pipetting. For this, five regions in each well (the four quadrants and center) were washed three times with 200 μl HBSS/$CaCl_2$ delivered using a stand-mounted pipette. Cells remaining adherent to the wells were then incubated with 10 mg/ml MTT dissolved in dimethylsulfoxide and read at $OD_{595}$ in a microplate reader. Cellular content in wells after pipetting was compared with the cellular content of wells prepared under identical conditions but not subjected to pipetting (yielding the total number of cells plated in each well).

### Plasmids

Porcine myosin VI–GFP and p–myosin VI–tail-GFP constructs were both gifts from T. Hasson (University of California, San Diego, La Jolla, CA;

Aschenbrenner et al., 2003). Plasmids encoding α-cat/vincHead, α-cat/vincTail, and α-catenin–HA were gifts from M. Watabe-Uchida and M. Takeichi (Kyoto University, Kyoto, Japan; Watabe-Uchida et al., 1998). To construct α-catenin bearing a C-terminal T7 tag, the HA tag of pCA-huaE-cat-HA-pA was replaced by cloning annealed oligonucleotides encoding the T7 tag into a unique Sal1 site. GFP-C1 control empty vector was purchased from CLONTECH Laboratories, Inc.

**Antibodies**

Primary antibodies used in this study are listed as follows: (1) a rabbit pAb (pAbMVI) directed against the whole tail domain of myosin VI was generated using a GST fusion protein (provided by F. Buss, University of Cambridge, Cambridge, UK; Buss et al., 1998). Approximately 250 μg of protein was used with Freud's adjuvant per injection to immunize rabbits. Immunoblotting cell lysates from several cell lines, including MCF-7 cells, with anti–myosin VI sera detected an intense band at the expected molecular mass of 140 kD as well as several other minor bands at lower molecular masses (that are possible degradation products), whereas naive rabbit sera from the same rabbit did not detect this band (Fig. S1, available at http://www.jcb.org/cgi/content/full/jcb.200612042/DC1)). Additionally, RNAi depletion of myosin VI resulted in loss of the band at 140 kD, and the re-expression of pMVIGFP restored this band at the expected molecular mass of 170 kD (Fig. 3 b). The other antibodies were obtained as follows: (2) mouse (mAb) HECD1 against human E-cadherin (a gift from P. Wheelock, University of Nebraska, Omaha, NE; with permission from M. Takeichi); (3) mouse mAb against GFP (Roche); (4) mouse mAb against human β-tubulin (Transduction Laboratories); (5) rabbit pAb against the ectodomain of E-cadherin (pAbE-cad; Helwani et al., 2004); (6) mouse mAb SHE78-7 against human E-cadherin (Zymed Laboratories); (7) mouse mAb against the cytoplasmic domain of E-cadherin (Transduction Laboratories); (8) rabbit pAb against human GAPDH (R&D Systems); (9) mouse mAb against human α-catenin (Transduction Laboratories); (10) mouse mAb against human p120-catenin (Transduction Laboratories); (11) rabbit pAb against human desmoplakin (a gift from K. Green, Northwestern University School of Medicine, Chicago, IL); (12) rabbit pAb against human ZO-1 (Zymed Laboratories); (13) mouse mAb against human vinculin (hVIN-1; Sigma-Aldrich); (14) mouse mAb against T7 tag (Novagen); and (15) rabbit pAb against GFP (Invitrogen). Secondary antibodies were species-specific antibodies conjugated with AlexaFluor350, 488, or 594 (Invitrogen) for immunofluorescence or were conjugated with HRP (Bio-Rad Laboratories) for immunoblotting.

**Immunofluorescence microscopy and image analysis**

To identify myosin VI, cells were incubated with prepermeabilization buffer (0.5% Triton X-100, 10 mM Pipes, pH 6.8, 50 mM NaCl, 3 mM $MgCl_2$, and 300 mM sucrose containing 1× complete protease inhibitors [Roche]) for 5 min on ice followed by fixation with 4% PFA in cytoskeletal stabilization buffer (100 mM KCl, 300 mM sucrose, 2 mM EGTA, 2 mM $MgCl_2$, and 10 mM Pipes, pH 7.2) for 10 min on ice. Otherwise, cells were fixed in PFA on ice for 10 min and were permeabilized. Fixed and stained specimens were mounted in either Mowiol (Calbiochem) or polyvinylalchohol mounting medium containing *N*-propylgallate (Sigma-Aldrich).

Epiillumination fluorescence microscopy of fixed specimens was performed at room temperature using a microscope (IX81; Olympus) with 100× or 60× 1.40 NA plan Apochromat objectives (Olympus) and imaged with cameras (Orca-1 ER; Hamamatsu) driven by MetaMorph imaging software (Universal Imaging Corp.). Confocal microscopy was performed at room temperature using a spinning disk confocal system (Ultra-View; PerkinElmer) mounted on a microscope (IX81; Olympus) with 100× or 60× 1.40 NA plan Apochromat objectives (Olympus) and a camera (Orca-1 ER; Hamamatsu) run with MetaMorph. Background correction and contrast adjustment of raw data images were performed with ImageJ (National Institutes of Health) or Photoshop (Adobe).

The intensity of E-cadherin and myosin VI fluorescence at cell–cell contacts was measured using the ImageJ tracing tool to identify contacts and quantitate the mean pixel intensity. Background was subtracted using a region with identical area for each contact quantitated. Experiments were performed four times with 40 contacts analyzed per experiment. To quantitate the differences in the continuity of contacts, the number of breaks within a contact were counted (contacts being defined as the regions between the vertices of two contiguous cells). Data shown are representative of four independent experiments.

**Antibody blocking, trypsin protection assay, and biotinylation**

MCF7 monolayers were incubated with function-blocking antibody SHE78-7 directed against the E-cadherin ectodomain at a 2-μg/ml concentration for 15–30 min. The surface expression of E-cadherin was measured by the sensitivity to surface trypsinization as described previously (Verma et al., 2004). Surface biotinylation was performed as previously described (Stehbens et al., 2006).

**Immunoprecipitation**

Cells were lysed in 1 ml of lysis buffer (50 mM Tris, pH 7.4, 2 mM $CaCl_2$, 150 mM NaCl, and 0.5% NP-40). Protein complexes were immunoprecipitated with anti–E-cadherin pAb, anti–myosin VI pAb, anti-GFP pAb, or a monoclonal vinculin mAb bound to protein A–agarose beads and were separated by SDS-PAGE. To coimmunoprecipitate α- and β-catenin with E-cadherin, the lysis buffer was 50 mM Tris, pH 7.4, 2 mM $CaCl_2$, 150 mM NaCl, and 1% NP-40; for p120-catenin, the buffer was 20 mM Hepes, 50 mM $CaCl_2$, 0.1 mM EDTA, and 1% NP-40.

**RNAi KD**

MCF7 monolayers seeded to 25% confluency were transfected with validated human myosin VI RNAi duplexes (5′-GGUUUAGGUGUUAAUGAAGtt-3′) and control duplexes (5′-GGUUUAGGUGUGAAUGAAGtt-3′; Ambion) at a 50-nM concentration using LipofectAMINE 2000 (Invitrogen) according to the manufacturer's guidelines. Cells were then replated at 25% confluency on day 3 after transfection and were allowed to incubate overnight before retransfection with 50 nM RNAi duplexes to ensure sustained KD. Cells were studied 24–48 h after the second plating. Vinculin RNAi was performed similarly with 100 nM of validated human vinculin RNAi duplexes (5′-GGCAUAGAGGAAGCUUUAAtt-3′) and mismatched controls (5′-GGCAUAGACCTTGCUUUAAtt-3′; Ambion).

**Online supplemental material**

Fig. S1 shows a characterization of the myosin VI antibody. Fig. S2 depicts the localization of myosin VI–GFP at cell–cell contacts. Fig. S3 quantitates the fluorescence intensity of myosin VI and E-cadherin at cell–cell contacts as cultures mature or when treated with cadherin-blocking antibodies. Fig. S4 shows the effect of myosin VI RNAi on cell adhesion to fibronectin. Fig. S5 depicts the effects of myosin VI KD on the expression of cadherin, catenins and vinculin, the cadherin–catenin complex, and the surface expression of cadherin. It also shows the effect of vinculin KD on levels of cadherin, catenins, and myosin VI. Online supplemental material is available at http://www.jcb.org/cgi/content/full/jcb.200612042/DC1.

We thank the many colleagues who provided reagents for this project, especially Tama Hassan, Folma Buss, Honami Naora, Mitsuko Watanabe-Uchida, Masatoshi Takeichi, and Robert Kypta. Our colleagues in the laboratory have, as always, been unfailing in their support, advice, and encouragement; we particularly thank Nicole den Elzen for her punctilious reading of the manuscript.

This work was supported by the Human Frontiers Science Program. M.P. Maddugoda is a Dora Lush Research Scholar of the Australian National Health and Medical Research Council (NHMRC), and A.S. Yap is an NHMRC Senior Research Fellow. A.S. Yap is a Research Affiliate of the Australian Research Council Special Research Centre for Functional and Applied Genomics, which provided infrastructure support for this work. Confocal microscopy was performed at the Australian Cancer Research Foundation (ACRF)/Institute for Molecular Bioscience Dynamic Imaging Facility for Cancer Biology, which was established with the support of the ACRF.

Submitted: 7 December 2006
Accepted: 3 July 2007

## References

Adams, C.L., Y.-T. Chen, S.J. Smith, and W.J. Nelson. 1998. Mechanisms of epithelial cell-cell adhesion and cell compaction revealed by high-resolution tracking of E-cadherin-green fluorescent protein. *J. Cell Biol.* 142:1105–1119.

Altman, D., H.L. Sweeney, and J.A. Spudich. 2004. The mechanism of myosin VI translocation and its load-induced anchoring. *Cell.* 116:737–749.

Aschenbrenner, L., T. Lee, and T. Hasson. 2003. Myo6 facilitates the translocation of endocytic vesicles from cell peripheries. *Mol. Biol. Cell.* 14:2728–2743.

Au, J.S., C. Puri, G. Ihrke, J. Kendrick-Jones, and F. Buss. 2007. Myosin VI is required for sorting of AP-1B-dependent cargo to the basolateral domain in polarized MDCK cells. *J. Cell Biol.* 177:103–114.

Bryant, D.M., and J.L. Stow. 2004. The ins and outs of E-cadherin trafficking. *Trends Cell Biol.* 14:427–434.

Buss, F., J. Kendrick-Jones, C. Lionne, A.E. Knight, G.P. Cote, and J. Paul Luzio. 1998. The localization of myosin VI at the golgi complex and leading edge of fibroblasts and its phosphorylation and recruitment into membrane ruffles of A431 cells after growth factor stimulation. *J. Cell Biol.* 143:1535–1545.

Buss, F., S.D. Arden, M. Lindsay, J.P. Luzio, and J. Kendrick-Jones. 2001. Myosin VI isoform localized to clathrin-coated vesicles with a role in clathrin-mediated endocytosis. *EMBO J.* 20:3676–3684.

Buss, F., J.P. Luzio, and J. Kendrick-Jones. 2002. Myosin VI, an actin motor for membrane traffic and cell migration. *Traffic*. 3:851–858.

Dawes-Hoang, R.E., K.M. Parmar, A.E. Christiansen, C.B. Phelps, A.H. Brand, and E.F. Wieschaus. 2005. Folded gastrulation, cell shape change and the control of myosin localization. *Development*. 132:4165–4178.

Geiger, B., K.T. Tokuyasu, A.H. Dutton, and S.J. Singer. 1980. Vinculin, an intracellular protein localized at specialized sites where microfilament bundles terminate at cell membranes. *Proc. Natl. Acad. Sci. USA*. 77:4127–4131.

Geisbrecht, E.R., and D.J. Montell. 2002. Myosin VI is required for E-cadherin-mediated border cell migration. *Nat. Cell Biol.* 4:616–620.

Goodwin, M., E.M. Kovacs, M.A. Thoreson, A.B. Reynolds, and A.S. Yap. 2003. Minimal mutation of the cytoplasmic tail inhibits the ability of E-cadherin to activate Rac but not phosphatidylinositol 3-kinase: direct evidence of a role for cadherin-activated Rac signaling in adhesion and contact formation. *J. Biol. Chem.* 278:20533–20539.

Gumbiner, B., B. Stevenson, and A. Grimaldi. 1988. The role of the cell adhesion molecule uvomorulin in the formation and maintenance of the epithelial junctional complex. *J. Cell Biol.* 107:1575–1587.

Hasson, T. 2003. Myosin VI: two distinct roles in endocytosis. *J. Cell Sci.* 116:3453–3461.

Helwani, F.M., E.M. Kovacs, A.D. Paterson, S. Verma, R.G. Ali, A.S. Fanning, S.A. Weed, and A.S. Yap. 2004. Cortactin is necessary for E-cadherin-mediated contact formation and actin reorganization. *J. Cell Biol.* 164:899–910.

Huttelmaier, S., P. Bubeck, M. Rudiger, and B.M. Jockusch. 1997. Characterization of two F-actin-binding and oligomerization sites in the cell-contact protein vinculin. *Eur. J. Biochem.* 247:1136–1142.

Ivanov, A.I., D. Hunt, M. Utech, A. Nusrat, and C.A. Parkos. 2005. Differential roles for actin polymerization and a myosin II motor in assembly of the epithelial apical junctional complex. *Mol. Biol. Cell*. 16:2636–2650.

Janssen, M.E., E. Kim, H. Liu, L.M. Fujimoto, A. Bobkov, N. Volkmann, and D. Hanein. 2006. Three-dimensional structure of vinculin bound to actin filaments. *Mol. Cell*. 21:271–281.

Jockusch, B.M., and G. Isenberg. 1981. Interaction of alpha-actinin and vinculin with actin: opposite effects on filament network formation. *Proc. Natl. Acad. Sci. USA*. 78:3005–3009.

Johnson, R.P., and S.W. Craig. 1995. F-actin binding site masked by the intramolecular association of vinculin head and tail domains. *Nature*. 373:261–264.

Johnson, R.P., and S.W. Craig. 2000. Actin activates a cryptic dimerization potential of the vinculin tail domain. *J. Biol. Chem.* 275:95–105.

Kovacs, E.M., M. Goodwin, R.G. Ali, A.D. Paterson, and A.S. Yap. 2002. Cadherin-directed actin assembly: E-cadherin physically associates with the Arp2/3 complex to direct actin assembly in nascent adhesive contacts. *Curr. Biol.* 12:379–382.

Kussel-Andermann, P., A. El-Amraoui, S. Safieddine, S. Nouaille, I. Perfettini, M. Lecuit, P. Cossart, U. Wolfrum, and C. Petit. 2000. Vezatin, a novel transmembrane protein, bridges myosin VIIA to the cadherin-catenins complex. *EMBO J.* 19:6020–6029.

Mege, R.M., J. Gavard, and M. Lambert. 2006. Regulation of cell-cell junctions by the cytoskeleton. *Curr. Opin. Cell Biol.* 18:541–548.

Menkel, A.R., M. Kroemker, P. Bubeck, M. Ronsiek, G. Nikolai, and B.M. Jockusch. 1994. Characterization of an F-actin-binding domain in the cytoskeletal protein vinculin. *J. Cell Biol.* 126:1231–1240.

Millo, H., K. Leaper, V. Lazou, and M. Bownes. 2004. Myosin VI plays a role in cell-cell adhesion during epithelial morphogenesis. *Mech. Dev.* 121:1335–1351.

Naccache, S.N., and T. Hasson. 2006. Myosin VI altered at threonine 406 stabilizes actin filaments in vivo. *Cell Motil. Cytoskeleton*. 63:633–645.

Noguchi, T., M. Lenartowska, and K.G. Miller. 2006. Myosin VI stabilizes an actin network during *Drosophila* spermatid individualization. *Mol. Biol. Cell*. 17:2559–2571.

Scott, J.A., A.M. Shewan, N.R. den Elzen, J.J. Loureiro, F.B. Gertler, and A.S. Yap. 2006. Ena/VASP proteins can regulate distinct modes of actin organization at cadherin-adhesive contacts. *Mol. Biol. Cell*. 17:1085–1095.

Shewan, A.M., M. Maddugoda, A. Kraemer, S.J. Stehbens, S. Verma, E.M. Kovacs, and A.S. Yap. 2005. Myosin 2 is a key Rho kinase target necessary for the local concentration of E-cadherin at cell-cell contacts. *Mol. Biol. Cell*. 16:4531–4532.

Stehbens, S.J., A.D. Paterson, M.S. Crampton, A.M. Shewan, C. Ferguson, A. Akhmanova, R.G. Parton, and A.S. Yap. 2006. Dynamic microtubules regulate the local concentration of E-cadherin at cell-cell contacts. *J. Cell Sci.* 119:1801–1811.

Tuxworth, R.I., I. Weber, D. Wessels, G.C. Addicks, D.R. Soll, G. Gerisch, and M.A. Titus. 2001. A role for myosin VII in dynamic cell adhesion. *Curr. Biol.* 11:318–329.

Vaezi, A., C. Bauer, V. Vasioukhin, and E. Fuchs. 2002. Actin cable dynamics and rho/rock orchestrate a polarized cytoskeletal architecture in the early steps of assembling a stratified epithelium. *Dev. Cell*. 3:367–381.

Verma, S., A.M. Shewan, J.A. Scott, F.M. Helwani, N.R. Elzen, H. Miki, T. Takenawa, and A.S. Yap. 2004. Arp2/3 activity is necessary for efficient formation of E-cadherin adhesive contacts. *J. Biol. Chem.* 279:34062–34070.

Walker, M.L., S.A. Burgess, J.R. Sellers, F. Wang, J.A. Hammer III, J. Trinick, and P.J. Knight. 2000. Two-headed binding of a processive myosin to F-actin. *Nature*. 405:804–807.

Warner, C.L., A. Stewart, J.P. Luzio, K.P. Steel, R.T. Libby, J. Kendrick-Jones, and F. Buss. 2003. Loss of myosin VI reduces secretion and the size of the Golgi in fibroblasts from Snell's waltzer mice. *EMBO J.* 22:569–579.

Watabe-Uchida, M., N. Uchida, Y. Imamura, A. Nagafuchi, K. Fujimoto, T. Uemura, S. Vermeulen, F. van Roy, E.D. Adamson, and M. Takeichi. 1998. α-Catenin–vinculin interaction functions to organize the apical junctional complex in epithelial cells. *J. Cell Biol.* 142:847–857.

Weiss, E.E., M. Kroemker, A.H. Rudiger, B.M. Jockusch, and M. Rudiger. 1998. Vinculin is part of the cadherin-catenin junctional complex: complex formation between alpha-catenin and vinculin. *J. Cell Biol.* 141:755–764.

Wells, A.L., A.W. Lin, L.Q. Chen, D. Safer, S.M. Cain, T. Hasson, B.O. Carragher, R.A. Milligan, and H.L. Sweeney. 1999. Myosin VI is an actin-based motor that moves backwards. *Nature*. 401:505–508.

Yamada, S., S. Pokutta, F. Drees, W.I. Weis, and W.J. Nelson. 2005. Deconstructing the cadherin-catenin-actin complex. *Cell*. 123:889–901.

Yamazaki, D., T. Oikawa, and T. Takenawa. 2007. Rac-WAVE-mediated actin reorganization is required for organization and maintenance of cell-cell adhesion. *J. Cell Sci.* 120:86–100.